

VU Research Portal

Hydrogen as a local probe: Diffusion and short-range order in $Ti_{1-y}V_y$ alloys

Brouwer, R.C.; Griessen, R.; Koeman, N.; Rector, J.

published in

Physical Review B. Condensed Matter
1989

document version

Publisher's PDF, also known as Version of record

[Link to publication in VU Research Portal](#)

citation for published version (APA)

Brouwer, R. C., Griessen, R., Koeman, N., & Rector, J. (1989). Hydrogen as a local probe: Diffusion and short-range order in $Ti_{1-y}V_y$ alloys. *Physical Review B. Condensed Matter*, 40(6), 3546-3559.

General rights

Copyright and moral rights for the publications made accessible in the public portal are retained by the authors and/or other copyright owners and it is a condition of accessing publications that users recognise and abide by the legal requirements associated with these rights.

- Users may download and print one copy of any publication from the public portal for the purpose of private study or research.
- You may not further distribute the material or use it for any profit-making activity or commercial gain
- You may freely distribute the URL identifying the publication in the public portal

Take down policy

If you believe that this document breaches copyright please contact us providing details, and we will remove access to the work immediately and investigate your claim.

E-mail address:

vuresearchportal.ub@vu.nl

Hydrogen as a local probe: Diffusion and short-range order in $Ti_{1-y}V_y$ alloys

R. C. Brouwer, J. Rector, N. Koeman, and R. Griessen

Natuurkundig Laboratorium, Vrije Universiteit te Amsterdam, NL-1081 HV Amsterdam, The Netherlands

(Received 31 January 1989; revised manuscript received 25 April 1989)

Diffusion coefficients of hydrogen have been measured in disordered $Ti_{1-y}V_y$ alloys, as a function of temperature, hydrogen concentration, and alloy composition. Diffusion and electron microprobe analysis data indicate the existence of short-range order (clustering) in $Ti_{1-y}V_y$ alloys, as observed before in the related $Ti_{1-y}Nb_y$ alloy system by diffusive x-ray scattering. The diffusion data are analyzed by means of a model, incorporating site-dependent activation energies, effective hydrogen-hydrogen interactions, and selective-blocking factors, generalized for alloys with short-range order. Site energies are calculated by means of the embedded-cluster model, assuming the energy of the hydrogen atoms to be predominantly determined by the nearest-neighbor metal atoms. An approximate relation between the short-range-order parameter σ and the site distribution is established. For $\sigma < 0$ a "chain" model and for $\sigma > 0$ a "cluster" model are in good agreement with Monte Carlo calculations. Using the short-range-order parameter σ as the only fit parameter, the short-range order in $Ti_{1-y}V_y$ alloys is determined from diffusion and solubility data. The quantitative determination of the short-range order in $Ti_{1-y}V_y$ alloys and $Mo_{1-y}Ti_y$ alloys from diffusion and solubility data, which are in excellent agreement with diffusive x-ray scattering data, shows that hydrogen can be a valuable tool to investigate the microscopic structure of concentrated disordered alloys.

I. INTRODUCTION

The solution and the diffusion of hydrogen and its isotopes, deuterium and tritium, in pure metals (e.g., V, Nb, Pd, Ni) at different temperatures (4–1200 K) and at different interstitial concentrations (0.001–200 at. %) have been studied extensively in the past decade.^{1–5} The observed phenomena are well understood and have been described, depending on the temperature regime, by quantum-mechanical or classical (rate) theories.^{1–5} However, first-principles calculations of, for example, the enthalpy of solution or the activation energy for diffusion of hydrogen in pure metals are still complicated, due to the high sensitivity of the properties of the interstitial atoms to the local structure of the metals.⁶

In the last few years research efforts moved gradually from hydrogen in pure metals to hydrogen in amorphous metals and (poly)crystalline alloys. Experimental results on *dilute* alloys were usually explained by two-stage-trapping models^{7,8} but in *concentrated* disordered alloys or amorphous metals distributions of sites with different energies have to be assumed.^{9,10} The existence of a site distribution in amorphous metals and (poly)crystalline alloys indicates that the energy of hydrogen on the interstitial sites is predominantly determined by the physical and chemical structure of the first shell (cluster) of neighboring metal atoms. The enthalpy of solution and the diffusion coefficients of interstitial atoms in the alloys depend strongly on the energy of the different sites (clusters) and on the fraction of sites with a given energy.^{11–13}

Recently, for the first time, it was shown that reliable site energies could be derived from detailed experimental pressure-composition data for hydrogen in a concentrat-

ed alloy system ($Nb_{1-y}V_y$ alloys).¹⁴ With the *same* site energies, the diffusion coefficients of hydrogen in the $Nb_{1-y}V_y$ alloys could be calculated as a function of temperature and hydrogen concentration, over the complete composition (y) range.¹¹ From the site energies in the $Nb_{1-y}V_y$ alloy system the average local distances Nb-Nb, Nb-V, and V-V were calculated and found to be in good agreement with local lattice separations predicted by the theory of Froyen and Herring.¹⁵

The results in the $Nb_{1-y}V_y$ alloy system showed for the first time convincingly that if the site energies and the site fractions are known then the enthalpy of solution and the diffusion coefficients of hydrogen in a concentrated alloy can be determined qualitatively, and in the case of $Nb_{1-y}V_y$ alloys even quantitatively. Conversely, one expects that experimental data for the enthalpy of solution and diffusion coefficients in some cases can be used to determine the site energies and the site fractions in an alloy. The site energies can then be related to local lattice parameters (as in the $Nb_{1-y}V_y$ alloys), and the site fractions can be related to the amount of short-range order in the alloy. In this way hydrogen can be used to obtain structural information in systems where the application of other techniques is difficult.^{16–18}

The purpose of this paper is to show that by measuring the enthalpy of solution and the diffusion coefficients of hydrogen in disordered alloys, it is possible to determine a further characteristic of an alloy (the amount of short-range order) beside site energies. As alloy system, we chose the $Ti_{1-y}V_y$ alloy system for the following reasons. For $y > 0.2$ the $Ti_{1-y}V_y$ alloys crystallize in the same bcc structure as $Nb_{1-y}V_y$ alloys. Both Nb and Ti have approximately the same molar volumes. Their affinity for hydrogen is, however, quite different as the molar enthal-

py of solutions at infinite dilution are -35.5 kJ/mol H for Nb and -55 kJ/mol H for Ti.^{1,19} Furthermore, there are clear indications of short-range order in the Ti_{1-y}V_y alloys.

First of all, Tanaka *et al.*²⁰ observed the formation of Ti clusters in V-rich alloys by electron microprobe analysis (EMPA), even in annealed samples but did not determine the short-range order quantitatively. In the somewhat comparable Ti_{1-y}Nb_y alloy system, short-range order has been observed by diffusive x-ray scattering, with a short-range-order parameter σ ranging between 0.1 and 0.15.²¹ Another indication for the existence of short-range order in Ti_{1-y}V_y alloys is the large scatter in experimental diffusion data. In Fig. 1 the apparent prefactor D_a^0 and the apparent activation energy for diffusion E_{act}^a are plotted as a function of alloy composition in Ti_{1-y}V_y alloys as found experimentally by various authors.^{20,22-24} The apparent prefactor and activation energy are obtained by fitting the expression $D^* = D_a^0 \exp(-E_{act}^a/RT)$ to experimental data for the chemical diffusion coefficient D^* of hydrogen in the alloy, i.e., by imposing a single site model to a system which is, in fact, characterized by a distribution of site energies and, consequently, activation energies. The systematic behavior of the activation energies E_{act}^a with anneal temperature (higher annealing temperatures yield lower E_{act}^a) indicated that the scatter in the experimental data is most probably caused by differences in the microscopic structure of the alloys, i.e., by different amounts of short-range order in the alloys.

This paper is organized as follows: In Sec. II a diffusion model incorporating site-dependent activation energies, selective-blocking factors, and interstitial-

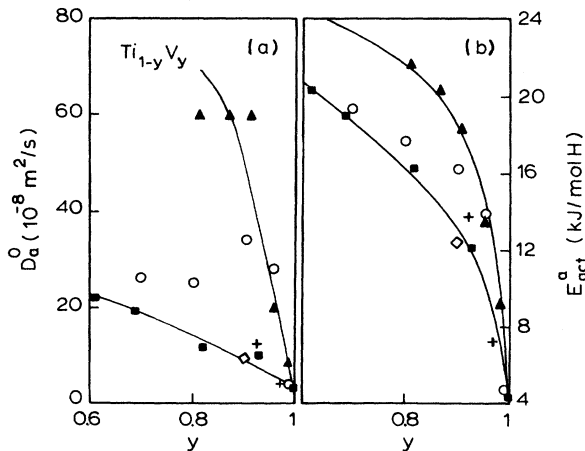


FIG. 1. Apparent prefactors D_a^0 , and activation energies E_{act}^a for diffusion of hydrogen in Ti_{1-y}V_y alloys as a function of alloy composition y . The apparent prefactors D_a^0 and activation energies E_{act}^a are defined by $D^* = D_a^0 \exp(-E_{act}^a/RT)$, with D^* the chemical diffusion coefficient. The large scatter in the experimental data indicates differences in the microscopic structure of the alloys, i.e., differences in short-range order (triangles, Ref. 20; circles, Ref. 22; pluses, Ref. 23; lozenge, Ref. 24; squares, this work). The lines are drawn as a guide for the eye.

interstitial interactions is presented. Important parameters in this model are the energies of the different sites and the number of sites with a given energy.

The *site energies* for hydrogen in Ti_{1-y}V_y alloys are calculated in Sec. III by the semi-empirical embedded cluster model. Recently the enthalpies of solution calculated with the embedded cluster model for Nb_{1-y}V_y, Cr_{1-y}V_y, Ta_{1-y}V_y, Ta_{1-y}Nb_y, and Mo_{1-y}Ti_y alloys were shown to be in excellent agreement with experimental data.²⁵

The *number of sites* with a given energy (site fraction) in an alloy with a random distribution of metal atoms, is simply given by a binomial distribution function. In alloys with short-range order, the site fractions depend on the amount of short-range order in the sample. Therefore, in Sec. IV the relations between the short-range order (parameter) in an alloy and the site fractions are derived, and compared with Monte Carlo calculations.

Diffusion coefficients for hydrogen in various Ti_{1-y}V_y alloys measured by means of the Gorsky effect as a function of temperature, hydrogen concentration and alloy composition are presented in Sec. V. Using the short-range order σ as the only fit parameter we determine σ both from existing solubility data and from diffusion coefficients for hydrogen in Ti_{1-y}V_y alloys. As we shall see, the values of σ determined in both ways are in good agreement with each other.

II. DIFFUSION IN DISORDERED ALLOYS

Until recently, diffusion of interstitial atoms at finite concentration in random alloys has attracted relatively little attention. McLellan and Yoshihara treated diffusion of interstitials in terms of a cell model in concentrated alloys, however, without accounting for blocking and interstitial-interstitial interactions.²⁶⁻²⁸ Kirchheim demonstrated in various papers the effects of site filling, blocking, correlation, and varying saddle-point energies in amorphous and deformed materials.²⁹⁻³¹

Brouwer *et al.*¹¹ proposed a model for interstitial diffusion in concentrated alloys taking into account site-dependent activation energies, interstitial-interstitial interactions, and selective-blocking factors. The diffusion coefficients calculated for the Nb_{1-y}V_yH_x system, as a function of temperature and hydrogen concentration appeared to be in excellent agreement with experimental diffusion data over the complete composition (y) range. In the following, a brief review of the physical concepts underlying this diffusion model will be given.

In a disordered alloy interstitial atoms occupy sites with different energies $\Delta\bar{H}_i(y)$. The probability that a site of type i is occupied is given by the following Fermi-Dirac distribution function, as multiple occupation of a given site is not allowed:^{9,10}

$$c_i = \frac{p_i}{s_i + \exp\{[\Delta\bar{H}_i(y) + f(c) - \mu]/RT\}} \quad (1)$$

with c_i the number of interstitial atoms, n_i , on sites of type i , divided by the total number of interstitial sites M , and p_i the number m_i of interstitial sites of type i , divided

TABLE I. Selective-blocking factors s_i for tetrahedral sites $A_{4-i}B_i$ in a bcc alloy $A_{1-y}B_y$. The probabilities p_{AAAA} , p_{AAAB} , etc., are defined in Sec. IV B. In an alloy $A_{1-y}B_y$ without short-range order $p_{ijkA} = 1-y$ and $p_{ijkB} = y$ where i, j, k can be either A or B . The blocking factors are valid up to $c \sim 0.04$ (24 at. % H).

i	Selective-blocking factors for clusters $A_{4-i}B_i$
0	$s_0 = 1 + \frac{3}{4}(4p_{AAAA})$
1	$s_1 = 1 + \frac{3}{4}(p_{AAAB} + 3p_{AABA})$
2	$s_2 = 1 + \frac{3}{4}(2p_{AABB} + 2p_{BBAA})$
3	$s_3 = 1 + \frac{3}{4}(p_{BBBA} + 3p_{BBAB})$
4	$s_4 = 1 + \frac{3}{4}(4p_{BBBB})$

by the total number of sites M ($c_i = n_i/M$ and $p_i = m_i/M$, thus c_i/p_i is the fractional occupation of sites of type i). The long-range interstitial-interstitial interaction $f(c)$ depends only on the total interstitial concentration c , with $c = \sum_i c_i$, for reasons discussed in Refs. 10 and 25.

The selective-blocking factor s_i is the number of sites of type i blocked by an interstitial atom on a site of type i . In a pure metal, s depends only on the interstitial concentration, and varies between 7 and 4 for hydrogen in a bcc metal. However, a good fit to experimental entropies is obtained by taking the limiting values of 4, indicating that at low concentrations the exact value of s in a pure metal is not important.³² In alloys the selective-blocking factors s_i depend on the type of site i , the alloy concentration, and the amount of short-range order in the alloy.¹¹ As an exact analytical solution is not possible, an approximation for the blocking factors in random bcc alloys has been proposed (for $c \leq 0.04$) in Ref. 11. These expressions are easily generalized for blocking in alloys with short-range order and are given in Table I.

In a disordered alloy the interstitial atoms jump from sites of type i to sites of type j , with an activation energy for diffusion $E_{ij}(c)$ depending on i and j . The chemical diffusion coefficient D^* becomes then

$$D^* = f_I \sum_i \sum_j D_{ij}^0 c_i q_{ij} \left[1 - \frac{s_j}{p_j} c_j \right] \times \exp[-E_{ij}(c)/RT] \frac{1}{RT} \frac{\partial \mu}{\partial c} \quad (2)$$

with q_{ij} the probability to find sites of type j next to sites of type i . This probability is not just p_j , the probability to find a site of type j in the alloy, but is determined by the crystal structure and the type of site i . In a bcc crystal, hydrogen atoms occupy tetrahedral interstitial sites. Two neighboring interstitial sites i and j have three metal atoms in common. Therefore, for a jump from a Ti_4 site to a V_4 site for example q_{ij} is zero. The values q_{ij} generalized for bcc alloys with short-range order are found in Table II. $1 - (s_j/p_j)c_j$ is the probability to find a free site j in the alloy.

The model cannot account explicitly for correlation effects. Correlation effects due to blocking and interactions at high interstitial concentration can be accounted for by f_I , which is also present in diffusion coefficients for the pure metals.³³⁻³⁵ In alloys correlation effects are, however, also expected if prefactors D_{ij}^0 and activation energies $E_{ij}(c)$ depend strongly on j . In this case care should be taken in the application of Eq. (2).

In order to use Eqs. (1) and (2) for the evaluation of our diffusion data the site energies $\Delta \bar{H}_i(y)$ have to be determined (Sec. III), and the relations between the site fractions p_i and the short-range-order parameter σ have to be established (Sec. IV).

III. SITE ENERGY: THE EMBEDDED CLUSTER MODEL

In order to calculate the chemical diffusion coefficients [Eq. (2)], we need to evaluate the site energies $\Delta \bar{H}_i(y)$. In Eq. (2) the fractional occupation, c_i , of sites of type i , depend on the site energy through Eq. (1). The activation energies for diffusion depend also on $\Delta \bar{H}_i(y)$, as $E_{ij} = Q_{ij} - \Delta \bar{H}_i(y)$ (see Fig. 3, Ref. 11).

As recently shown for the $Nb_{1-y}V_y$ alloy system^{14,36} site energies can be determined by measuring pressure-composition isotherms of hydrogen in the alloys, but with regard to the almost infinite number of alloys, this is not a very practical method.

As first-principles calculations proved to be inaccurate,^{37,38} the best way to calculate site energies in alloys, is to use the semiempirical local band-structure model. The enthalpy of solution of hydrogen in transition metals at infinite dilution $\Delta \bar{H}_\infty$ (in kJ/mol H) was shown to obey the relation³⁹

$$\Delta \bar{H}_\infty = \alpha \Delta E W_d^{1/2} \sum_j R_j^{-4} + \beta \quad (3)$$

TABLE II. Probability q_{ij} to find a site $A_{4-j}B_j$ as nearest-neighbor site of a given site $A_{4-i}B_i$ in an alloy $A_{1-y}B_y$. The probabilities p_{AAAA} , p_{AAAB} , etc., are defined in Sec. IV B. In an alloy $A_{1-y}B_y$ without short-range order $p_{ijkA} = 1-y$ and $p_{ijkB} = y$, where i, j, k can be either A or B .

$A_{4-i}B_i$ \ $A_{4-j}B_j$	B_4	AB_3	A_2B_2	A_3B	A_4
B_4	p_{BBBB}	p_{BBBA}	0	0	0
AB_3	$\frac{1}{4}p_{BBBB}$	$\frac{1}{4}p_{BBBA} + \frac{3}{4}p_{BBAB}$	$\frac{3}{4}p_{BBAA}$	0	0
A_2B_2	0	$\frac{1}{2}p_{BBAB}$	$\frac{1}{2}p_{AABB} + \frac{1}{2}p_{BBAA}$	$\frac{1}{2}p_{AABA}$	0
A_3B	0	0	$\frac{3}{4}p_{AABB}$	$\frac{1}{4}p_{AAAB} + \frac{3}{4}p_{AABA}$	$\frac{1}{4}p_{AAAA}$
A_4	0	0	0	p_{AAAB}	p_{AAAA}

with $\alpha = 18.6 \text{ kJ/mol H } (\text{\AA}^4 \text{ eV})^{-3/2}$ and $\beta = -90 \text{ kJ/mol H}$ and $\Delta E, W_d$ in eV and R_j in \AA . ΔE is a characteristic band-structure energy $\Delta E = E_F - E_s$, with E_F the Fermi energy and E_s the center of the lowest conduction band of the host metal. W_d is the d -band width of the host metal and R_j the distance between a given hydrogen atom and the j th neighboring metal atom.

In the embedded cluster model the site energies, $\Delta \bar{H}_i(y)$, in a bcc alloy $A_{1-y}B_y$ are assumed to depend predominantly on the cluster $A_{4-i}B_i$ of nearest-neighbor metal atoms (assuming occupancy of the tetrahedral interstitial sites). The cluster $A_{4-i}B_i$ (with $i=0, 1, \dots, 4$) is treated as an alloy with (local) concentration $y' = i/4$. The enthalpy of solution, i.e., the site energy $\Delta \bar{H}_i(y)$, is then calculated by Eq. (3) for the free cluster $A_{4-i}B_i$ (or equivalently for the alloy with $y' = i/4$), using the appropriate values ΔE_i^* and W_i^* . As in most cases characteristic band-structure parameter ΔE_i^* and the bandwidth W_i^* are not known for alloys the procedure proposed by Cyrot and Cyrot-Lackmann is used to calculate these parameters from the band-structure parameters of the pure metals A and B .^{25,40,41}

The site energy of the free cluster $A_{4-i}B_i$, $\Delta \bar{H}_i$, is then calculated by substituting W_i^* and ΔE_i^* in Eq. (3). In reality the cluster $A_{4-i}B_i$ is embedded in the matrix of the alloy $A_{1-y}B_y$. The site energy, $\Delta \bar{H}_i$, is calculated for a cluster $A_{4-i}B_i$ with local volume

$$\Omega_i = \frac{(4-i)\Omega_A + i\Omega_B}{4} \quad (4)$$

with Ω_A and Ω_B the cluster volume of A_4 and B_4 in the pure metals. The average cluster volume $\bar{\Omega}(y)$ in the alloy, however, is given by

$$\bar{\Omega}(y) = (1-y)\Omega_A + y\Omega_B \quad (5)$$

The actual volume $\Omega_i(y)$ of the embedded cluster $A_{4-i}B_i$ is intermediate between the volume of a free cluster Ω_i and the average cluster volume $\bar{\Omega}(y)$ and can be expressed as

$$\Omega_i(y) = (1-D)\bar{\Omega}(y) + D\Omega_i \quad (6)$$

For $D=0$ the lattice of the alloy is free of distortions and the volume of each cluster $A_{4-i}B_i$ is equal to the average volume. For $D=1$ the cluster is not at all influenced by the surrounding lattice. The parameter D is related to the parameter I_1 in the work of Froyen and Herring¹⁵ by²⁵

$$D = 1.58I_1 \quad (7)$$

I_1 can be determined from Fig. 1 of Ref. 15 once the elastic constants c_{11} , c_{12} , and c_{44} are known. The site energy $\Delta \bar{H}_i(y)$ of the embedded cluster $A_{4-i}B_i$ in the alloy $A_{1-y}B_y$ is finally obtained from

$$\Delta \bar{H}_i(y) = \Delta \bar{H}_i - \frac{B\bar{V}_H}{V_m} [\Omega_i(y) - \Omega_i] \quad (8)$$

with V_m the molar volume of the alloy, B the bulk modulus, and \bar{V}_H the molar volume of hydrogen in the al-

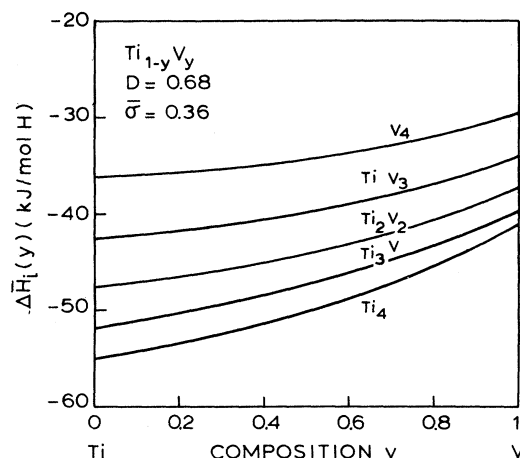


FIG. 2. Site energies $\Delta \bar{H}_i(y)$ for $\text{Ti}_{1-y}\text{V}_y$ alloys as a function of alloy composition. Curves are drawn for $D = 0.68$, calculated from the elastic constants, and for $\bar{\sigma} = 0.36$, the average short-range order found in the $\text{Ti}_{1-y}\text{V}_y$ alloys from the diffusion data.

loy. Equation (8) follows directly from the fact that $d\Delta \bar{H}_i/d \ln V = -B\bar{V}_H$.^{14,42} The embedded cluster model presented above was used to calculate the enthalpy of solution in $\text{Nb}_{1-y}\text{V}_y$, $\text{Cr}_{1-y}\text{V}_y$, $\text{Ti}_{1-y}\text{V}_y$, $\text{Mo}_{1-y}\text{Ti}_y$, $\text{Ta}_{1-y}\text{V}_y$, and $\text{Ta}_{1-y}\text{Nb}_y$ alloys as a function of hydrogen concentration and alloy composition.²⁵ An excellent agreement with experimental data was obtained for all these alloy systems using calculated values [from elastic constants via Eq. (7)] for the parameter D .

In Fig. 2 the calculated site energies for the $\text{Ti}_{1-y}\text{V}_y$ alloy system are plotted for $D = 0.68$. This value for D was determined from experimental data on the elastic constants for $\text{Ti}_{1-y}\text{V}_y$ alloys with $0.3 \leq y \leq 1$.⁴³ The Ti_4 sites have the lowest energy and by alloying V to Ti the site energy increases due to the decreasing site volumes. Due to the small bulk modulus in these Ti alloys, a change in site volume results in a relatively small change in $\Delta \bar{H}_i(y)$. Furthermore, as we shall discuss in detail in the next section, in $\text{Ti}_{1-y}\text{V}_y$ alloys short-range-order effects are observed. Ti and V atoms tend to form clusters of like atoms. The local Ti concentration around a Ti_4 cluster is thus larger than the average Ti concentration in the alloy. Consequently, there is an increased tendency for Ti_4 sites to retain the volume of a Ti_4 cluster in pure Ti.

In order to use the site energies and Eq. (2) to calculate diffusion coefficients (Sec. V) the influence of short-range order on $\Delta \bar{H}_i(y)$ and the relations between the short-range-order parameter and the fraction of sites of a certain type p_i have to be established.

IV. SHORT-RANGE ORDER

In a random bcc alloy, with interstitial atoms on the tetrahedral sites, the fraction of sites of a certain type is given by the binomial distribution

$$p(i, \sigma=0) = \binom{4}{i} (1-y)^{4-i} y^i \quad (9)$$

for sites $A_{4-i}B_i$ in the alloy $A_{1-y}B_y$. The short-range-order parameter σ , which is by definition zero for a random distribution of metal atoms, is defined by the following pair probabilities (with $p_A = 1-y$ and $p_B = y$):^{13,44}

$$p_{AA} = p_A + (1-p_A)\sigma, \quad (10a)$$

$$p_{AB} = p_B - p_B\sigma, \quad (10b)$$

where p_{AA} is the probability to find an A atom as nearest neighbor of another A atom. The pair probabilities are related to each other by

$$p_{AA} + p_{AB} = 1, \quad (11a)$$

$$p_{AA}p_{AB} - p_{BB}p_{BA} = 0. \quad (11b)$$

[Relations for p_{BA} and p_{BB} are obtained by exchanging A and B in Eqs. 10(a), 10(b), and 11(a).] For $\sigma > 0$, the A and B atoms form clusters of like atoms while for $\sigma < 0$ ordered structures, compounds, are formed.

The chemical diffusion coefficients for hydrogen in an alloy with short-range order [Eq. (2)] depend on the site fractions p_i and, consequently, on the short-range order σ . If we can establish functional relations between σ (related to the pair probability) and the probabilities to find certain clusters in the alloy, p_i , then we are able to calculate D^* if σ is known, or, conversely, we can determine the short-range order σ from a one-parameter fit to our diffusion data. As exact relations between σ and p_i cannot be derived, we shall search for approximate solutions, and compare them with Monte Carlo calculations.

In Sec. IV A a simple linear, "chain," model is derived and the influence of the short-range order on the local volumes, and consequently the site energies, is discussed [Eqs. (6) and (8)]. Comparing the chain model with Monte Carlo calculations in part C, an excellent agreement is obtained for $\sigma < 0$. For $\sigma > 0$, however, a more refined model, the "cluster" model, derived in Sec. III B, gives a better agreement with the Monte Carlo data.

A. The chain model

The simplest approximation is to consider a cluster $A_{4-i}B_i$ as a linear chain of atoms. The probability to find an A_4 site in the alloy $A_{1-y}B_y$, is then the probability to form an $AAAA$ chain of atoms

$$p(i=0, \sigma) = p_A p_{AA}^3. \quad (12a)$$

The probability to find the first A atom is just p_A , the next A atom p_{AA} , etc. The equations for the other clusters are derived in an analogous way,

$$p(i=1, \sigma) = p_A p_{AA}^2 p_{AB} + 2p_A p_{AA} p_{AB} p_{BA} + p_B p_{BA} p_{AA}^2, \quad (12b)$$

$$\begin{aligned} p(i=2, \sigma) = & p_A p_{AA} p_{AB} p_{BB} + p_A p_{AB} p_{BA} p_{AB} \\ & + p_A p_{AB} p_{BB} p_{BA} + p_B p_{BA} p_{AA} p_{AB} \\ & + p_B p_{BA} p_{AB} p_{BA} + p_B p_{BB} p_{BA} p_{AA}, \end{aligned} \quad (12c)$$

[$p(i=3, \sigma)$ and $p(i=4, \sigma)$ are obtained from $p(i=1, \sigma)$ and $p(i=0, \sigma)$ by exchanging A and B] where a summation is made over all possible ways to form a chain of 4 atoms. In the actual lattice there are six bonds between the atoms in a tetrahedron, while in the chain model only three bonds are considered. Therefore, for $\sigma > 0$ (clustering) the actual number of A_4 or B_4 sites is expected to be larger than the number predicted by the chain model. This is confirmed by Monte Carlo calculations (in Sec. III C).

The local volumes defined in Eq. (6) will also be influenced by the amount of short-range order σ . Consider, for example, Ti_4 clusters in a $Ti_{1-y}V_y$ alloy surrounded by a large cluster of Ti atoms. These clusters will have a larger volume than Ti_4 sites surrounded by a random distribution of atoms in the lattice. In the chain model the average lattice concentration around a cluster depends on the ends of the chain. Considering an A_3B site ($-AAA-$, $-AABA-$, $-ABAA-$, $-BAAA-$) the probability to find an A atom next to the cluster is approximated by

$$p_A = \frac{1}{4}p_{BA} + \frac{3}{4}p_{AA} \quad (13)$$

and p_A is then the average concentration around the cluster. Substituting p_A for y in Eq. (6), for all clusters, we obtain

$$\Omega_i(y) = [(1-y)\Omega_A + y\Omega_B](1-D') + D'\Omega_i \quad (14)$$

with $D' = D + (1-D)\sigma$, and σ interpolates D' simply between D and 1 (complete segregation).

B. The cluster model

The cluster model (for $\sigma > 0$) incorporates all six bonds found in a tetrahedron. Consider for example an A_4 cluster. The probabilities to find the first and second A atom are simply p_A and $p_{AA}(\sigma)$, respectively [see Eq. (10a)]. The short-range-order parameter σ may be viewed as an interpolation for $p_{AA}(\sigma)$ between p_A and 1. Consider now a third A atom to be placed in the cluster. The probability for this third atom, $p_{AAA}(\sigma)$, must be at least $p_{AA}(\sigma)$ and at most be 1. The natural extension of Eq. (10a) is then

$$p_{AAA} = p_{AA} + (1-p_{AA})\sigma \quad (15)$$

and the probability for the fourth A atom is analogously

$$p_{AAAA} = p_{AAA} + (1-p_{AAA})\sigma. \quad (16)$$

The probability to find an A_4 cluster in the alloy is thus given by

$$p(i=0, \sigma) = p_A p_{AA} p_{AAA} p_{AAAA}. \quad (17a)$$

The analogous expressions for the formation of the other clusters are

$$\begin{aligned}
 p(i=1, \sigma) = & p_{APAAPAAAPAAAB} + p_{APAAPAABPAAAB} \\
 & + p_{APABPABAPABAA} + p_{BPBAPBAAAPBAAA}, \quad (17b)
 \end{aligned}$$

$$\begin{aligned}
 p(i=2, \sigma) = & p_{APAAPAABPAAAB} + p_{APABPABAPABAB} \\
 & + p_{BPBAPBAAAPBAAAB} + p_{BPBAPBAPBAPBABA} \\
 & + p_{BPBAPBAPBAAAPBAAA} + p_{APABPABPABPABBA}, \quad (17c)
 \end{aligned}$$

[$p(i=3, \sigma)$ and $p(i=4, \sigma)$ are obtained from $p(i=1, \sigma)$ and $p(i=0, \sigma)$ by exchanging A and B]. The probability p_{AAAB} corresponds to the chance to find a B atom next to three A atoms. This must be

$$\begin{aligned}
 p_{AAAB} &= 1 - p_{AAAA} \\
 &= p_B - p_B(3\sigma - 3\sigma^2 + \sigma^3), \quad (18)
 \end{aligned}$$

which expresses the influence of three A atoms in an analogous way as for one A atom in p_{AB} [Eq. (10b)]. The probability to find a B atom next to two A atoms and one B atom is p_{BAB} (or p_{BAA}). The B atom already in the cluster increases (for $\sigma > 0$) the probability to find another B atom, the two A atoms decrease it. The approximation is made that the influence of one A and B atom cancel each other, and therefore

$$p_{BAA} = p_{AB} = p_B - p_B \sigma. \quad (19)$$

The other probabilities in Eqs. (17a)–(17c) are now easily derived (see Appendix).

C. Comparison with Monte Carlo calculations

In the chain model and the cluster model, the probability to find a single chain or cluster of atoms is calculated.

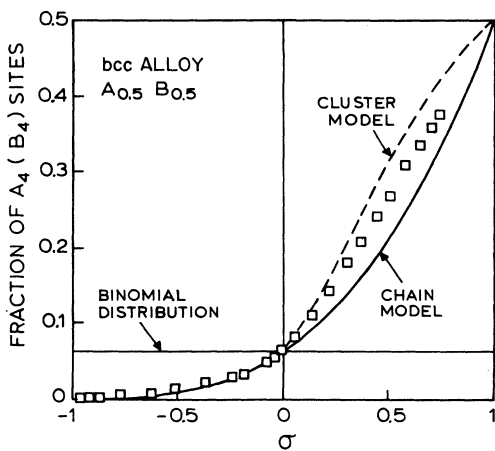


FIG. 3. Relation between the short-range-order parameter σ and the fraction of A_4 (B_4) sites in a bcc $A_{0.5}B_{0.5}$ alloy. The binomial distribution ($\sigma=0$) is given by the horizontal line. The solid curve is calculated with the chain model, the dashed line with the cluster model. The squares are Monte Carlo points. For $\sigma=-1$ a complete ordering occurs and the number of A_4 (B_4) sites vanishes. For $\sigma=1$ phase separation occurs and the alloy consists only of A_4 and B_4 sites.

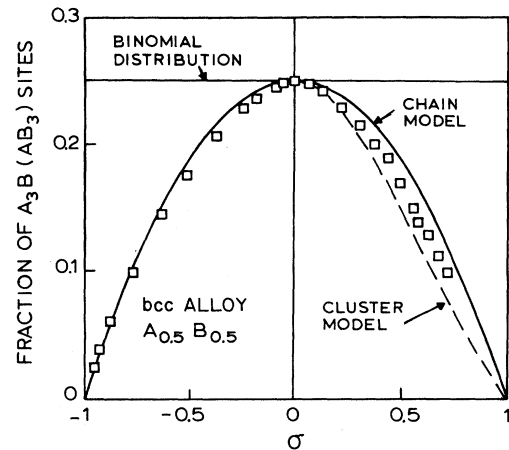


FIG. 4. Relation between the short-range-order parameter σ and the fraction of A_3B (AB_3) sites in a bcc $A_{0.5}B_{0.5}$ alloy. The Monte Carlo points (squares) for $\sigma > 0$ are in between the cluster model (dashed line) and the chain model (solid curve).

In the real lattice, the chains or clusters are influenced by other chains or clusters. The probability to find a certain cluster (site) is a three-dimensional problem, which depends strongly on the crystal structure of the metal. An exact analytical solution for the site fractions as a function of the short-range-order parameter is not possible. In order to check the validity of the chain and cluster approximation presented above we also established the relation between σ and p_i by Monte Carlo calculations on bcc alloys $A_{1-y}B_y$ as a function of alloy composition. As we are only interested in a statistical relation between the number of pairs (σ) and the number of clusters [$p(i, \sigma)$], the Monte Carlo calculations will not be discussed in detail here.

In Figs. 3–5 the site fractions for an $A_{0.5}B_{0.5}$ alloy are

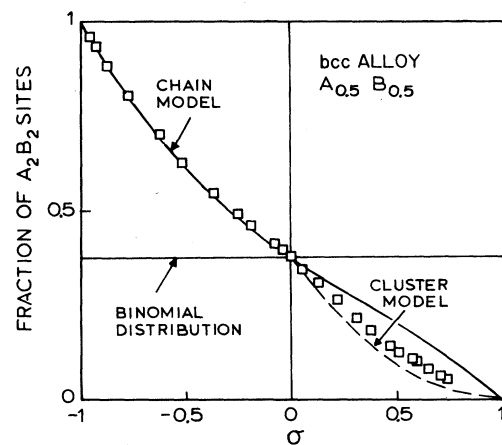


FIG. 5. Relation between the short-range-order parameter σ and the fraction of A_2B_2 sites in a bcc $A_{0.5}B_{0.5}$ alloy. For $\sigma=-1$ ordering occurs and only A_2B_2 sites exist. For $\sigma=1$ phase separation occurs and the number of A_2B_2 sites vanishes. The Monte Carlo points (squares) are in between the cluster model (dashed line) and the chain model (solid curve) for $\sigma > 0$.

plotted as a function of the amount of short-range order σ for the binomial distribution (horizontal line), the chain model (solid curve), the cluster model (dashed curve), and the Monte Carlo calculations (squares).

For $\sigma < 0$ the predictions of the chain model are in excellent agreement with the Monte Carlo calculations. For $\sigma > 0$ the deviations from the binomial distribution predicted by the chain model are slightly too small, probably because only three bonds are considered. In contrast, the cluster model predicts a deviation from the binomial distribution which is slightly too high. Monte Carlo calculations for $y=0.1$ showed for $\sigma < 0$ again an excellent agreement with the chain model, while for $\sigma > 0$ a good agreement with the cluster model is obtained. For this alloy composition the chain model results in deviations (if $\sigma > 0.2$) for A_2B_2 and A_1B_3 sites.

Therefore, we conclude that for $\sigma < 0$ the chain model and for $\sigma > 0$ the cluster model should be used to calculate the site fractions as a function of the short-range-order parameter σ .

V. EXPERIMENTS

The site energies $\Delta\bar{H}_i(y)$ entering Eq. (2) were calculated in Sec. III, the relations between the site fractions p_i and σ were established in Sec. IV. Now we are able to calculate D^* , using Eq. (2), as a function of temperature, hydrogen concentration and alloy composition in an alloy with short-range order. The short-range order σ is used as a fit parameter in a comparison with experimental diffusion coefficients.

In Sec. V A, the sample preparation is described in detail, as the amount of short-range order in the $Ti_{1-y}V_y$ alloys depends on the temperature treatment of the samples. In Sec. V B the enthalpy of solution of hydrogen in $Ti_{1-y}V_y$ alloys, $\Delta\bar{H}(y)$, is calculated and compared with existing experimental data. In Secs. V C and V D diffusion data are presented as a function of temperature, hydrogen concentration, and alloy composition.

A. Sample preparation

Several authors^{20,45} have reported on the formation of Ti and V clusters in $Ti_{1-y}V_y$ alloys due to attractive interactions between like atoms. As the short-range order in alloys depends on the sample preparation, the temperature treatment of our samples is described in detail.

The $Ti_{1-y}V_y$ alloys used in the diffusion experiments

are prepared from Marz grade Ti and V with a purity of 99.95 at. %. First the Ti and V slugs are melted together, and remelted several times by high-frequency (HF) heating in an argon atmosphere (weight losses $\sim 0.01\%$). After casting the samples into a cylindrical form in an electron gun (weight loss $\sim 1\%$), the samples are annealed for 8 h at 100 K below the melting point by HF heating in an argon atmosphere. Contaminations in the argon gas are gettered by sublimating Ti on a metal foil. The samples are allowed to cool down by radiation and heat conduction of the argon gas, and are cut to the desired dimensions (typically $24 \times 3 \times 0.5$ mm) by spark erosion. All samples are analyzed with an electron microprobe (EMP) and by x-ray diffraction to determine their homogeneity and crystal structure.^{46,47} In order to obtain some information on the influence of the annealing temperature and annealing time on the (in)homogeneity of the $Ti_{1-y}V_y$ alloys, a number of $Ti_{0.38}V_{0.62}$ samples are annealed at 1370 K for 72 h and at 1820 K for 8, 16, and 30 h. Not-annealed samples show a typical variation in the Ti concentration of ~ 3 at. %; samples annealed at 1370 K show no improvement in homogeneity, but samples annealed at 1820 K are all found to be homogeneous within the resolution of the EMP (the EMP has a concentration resolution of 0.2 at. % on a spot of $3 \mu\text{m}$). These results are qualitatively in agreement with the result of Tanaka and Kumura²⁰ who annealed their samples at 1270 K for 29 h and found a 1 at. % Ti variation in a $Ti_{1-y}V_y$ alloy containing 5 at. % Ti. The annealing temperature, annealing time, Ti and V concentrations, and the (in)homogeneity of our samples, as determined by EMP analysis are tabulated in Table III.

B. The enthalpy of solution in $Ti_{1-y}V_y$ alloys

Before considering the diffusion experiments we calculate the enthalpy of solution of hydrogen $\Delta\bar{H}(y)$ as a function of alloy composition for $Ti_{1-y}V_y$ alloys and compare the calculated $\Delta\bar{H}(y)$ with existing experimental data. The enthalpy of solution can be calculated using¹³

$$\Delta\bar{H}(y) = f(c) + \frac{\sum_i \Delta\bar{H}_i(y)c_i \left[1 - \frac{s_i}{p_i}c_i \right]}{\sum_i c_i \left[1 - \frac{s_i}{p_i}c_i \right]}, \quad (20)$$

where $f(c)$ is the long-range effective hydrogen-hydrogen interaction, $\Delta\bar{H}_i(y)$ are the site energies, c_i the concentra-

TABLE III. Annealing temperature T_a , annealing time t_a , Ti and V concentrations determined from EMP data, and the homogeneity in at. % V of the samples used in the diffusion experiments.

Sample	T_a (K)	t_a (h)	Ti at. %	V at. %	Δc (at. % V)
$Ti_{0.07}V_{0.93}$	1970	6.5	7.12	92.88	0.15
$Ti_{0.18}V_{0.82}$	1920	6.5	18.23	81.77	0.3
$Ti_{0.31}V_{0.69}$	1908	8	30.90	69.10	0.25
$Ti_{0.38}V_{0.62}$	1870	7	38.50	61.50	0.3

TABLE IV. Data used in calculating the site energies in the Ti_{1-y}V_y alloys. From left to right in columns, the symbol of the element, the molar volume V_m , the enthalpy of solution for hydrogen at infinite dilution $\Delta\bar{H}_\infty$, the band-structure parameter $\Delta E = E_F - E_S$, the d -band width W_d , the density of states at the Fermi level $n(E_F)$, the work function Φ , the parameter D defined in Eq. (6), the optimized values $\Delta E^0 = \lambda \Delta E$, and $W_d^0 = \lambda W_d$ with λ determined from the condition that $\Delta\bar{H}_\infty = \alpha \Delta E W_d^{1/2} \lambda^{3/2} \sum_j R_j^{-4} + \beta$ reproduces exactly the measured heat of solution of hydrogen in the pure metals.

	V_m^a (cm ³ /mol)	$\Delta\bar{H}_\infty^b$ (kJ/mol H)	ΔE^c (eV)	W_d^c (eV)	$n(E_F)^d$ states/atom	Φ^e (eV)	D^f	ΔE^0 (eV)	W_d^0 (eV)
V	8.35	-29.5	2.90	6.6	1.64	4.3	0.59	2.69	6.13
β -Ti	10.6	-55	2.45	6.6	1.59	4.33	0.68	2.18	5.89

^aFrom Reference 42.

^bFrom References 19 and 36.

^cFrom Reference 39.

^dFrom Reference 54.

^eFrom Reference 56.

^fFrom References 15 and 43.

TABLE V. Bulk modulus B , molar volume \bar{V}_H , parameters A_1^c and A_i ($i=1, 2, 3$, and 4) in kJ/mol H entering the expressions for the calculated effective H-H interaction $f^c(c) = A_1^c c$ and the experimentally determined H-H interaction $f(c) = A_1 c + A_2 c^2 + A_3 c^3 + A_4 c^4$. The concentration c is given by the total number of hydrogen atoms, N , divided by the total number of interstitial sites, M .

	B^c (kJ/cm ³)	\bar{V}_H^b (cm ³ /mol H)	A_1^c (kJ/mol H)	A_1^a (kJ/mol H)	A_2 (kJ/mol H)	A_3 (kJ/mol H)	A_4 (kJ/mol H)
V	157	1.59	-202	-222	4.35×10^3	-7.78×10^4	5.55×10^5
β -Ti	95	1.6	-77	-60			

^aReferences 19 and 36.

^bReferences 1 and 19.

^cReference 55.

TABLE VI. Experimental data for various alloys. From left to right in the columns, alloy composition, hydrogen concentration $c = N/M$, apparent prefactor D_a^0 , apparent activation energy for diffusion E_{act}^a , the prefactor D^0 obtained from fitting Eq. (2) to the experimental data, the saddle-point energy Q , short-range-order parameter σ determined from diffusion data, and σ determined from the enthalpy of solution in Fig. 6.

Alloy	c	D_a^0 (10^{-8} m ² /s)	E_{act}^a (kJ/mol H)	D^0 (10^{-8} m ² /s)	Q (kJ/mol H)	σ Diffusion	σ Solution
V	0.001	3.1	4.5	3.1	-25.2	0	0
Ti _{0.07} V _{0.93}	0.0020	9.9	12.1	3.4	-25.7	0.41	0.44
	0.0092	7.0	11.6	3.4	-25.7	0.41	
	0.0187	7.3	12.4	3.4	-25.7	0.41	
	0.0325	9.5	14.1	3.4	-25.7	0.41	
Ti _{0.18} V _{0.82}	0.0026	11.6	16.2	4.0	-25.7	0.40	0.40
	0.0110	8.2	15.0	4.0	-25.7	0.40	
Ti _{0.31} V _{0.69}	0.0033	19.2	19.0	8.3	-25.7	0.34	0.33
Ti _{0.38} V _{0.62}	0.0028	21.9	20.3	9.0	-25.7	0.32	
	0.0081	10.8	18.3	9.0	-25.7	0.32	
	0.0247	9.2	17.4	9.0	-25.7	0.32	
β -Ti	0.001	19.5	27.8	19.5	-27.2	0	0

tions of hydrogen on sites of type i , s_i the blocking factors, and p_i the site fractions. The blocking factors¹¹ are determined from Table I and depend on the short-range order σ . The site distribution p_i depends on the short-range-order parameter σ via Eqs. (12a)–(12c) or (17a)–(17c). The interaction $f(c)$ depends only on the total hydrogen concentration. It can be calculated using the semi-empirical local band-structure model, Eq. (3), by

$$f^c(c) = \int_0^c \left[-\frac{B\bar{V}_H^2}{V_m} + \frac{\alpha v W_d^{1/2}}{n(E_F)} \sum_j R_j^{-4} \right] dc \quad (21)$$

The effective hydrogen-hydrogen interactions $f^c(c)$ are calculated in first order for the pure metals V and Ti using the (optimized) band-structure parameters in Table IV. The calculated interactions $f^c(c)$ are compared with experimental data in Table V. The (first-order) calculated interaction terms $f^c(c) = A^c c$ are in agreement with the experimental values, both for V and β -Ti.

In alloys the long-range H-H interactions $f(c)$ do not depend on local site energies and in $\text{Nb}_{1-y}\text{V}_y$, $\text{Cr}_{1-y}\text{V}_y$, and $\text{Ta}_{1-y}\text{Nb}_y$ alloys a good agreement with experimental enthalpies of solution was obtained up to high hydrogen concentrations by simply interpolating $f(c)$ between the values of the pure metals.²⁵ Therefore, and because most parameters in Eq. (21) are indeed expected to interpolate smoothly between Ti and V, we simply take a linear interpolation for $f(c)$ between pure V and β -Ti. The site energies $\Delta\bar{H}_i(y)$ are calculated by the embedded cluster model in Sec. III, and are assumed to depend on σ via Eq. (14).

Now we have assigned values to all parameters in Eq. (20), and they only depend on the short-range order σ . In Fig. 6 the enthalpies of solution determined by Peterson *et al.*⁴⁸ for hydrogen in $\text{Ti}_{1-y}\text{V}_y$ alloys are plotted as a function of alloy composition at 385 K and for $c = 0.01$ (6 at. % H).

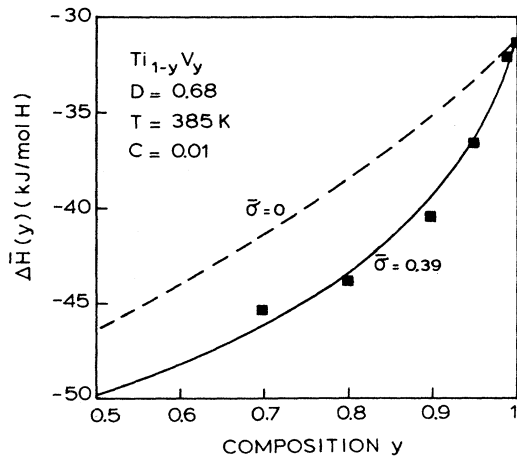


FIG. 6. Enthalpy of solution $\Delta\bar{H}(y)$ for hydrogen in $\text{Ti}_{1-y}\text{V}_y$ alloys at 385 K, $c = 0.01$ and $D = 0.68$ [defined by Eq. (16)], as a function of composition. The dashed curve is calculated with $\bar{\sigma} = 0$, and the solid curve with $\bar{\sigma} = 0.39$. The squares are experimental data from Ref. 48.

The short-range order is determined for each alloy separately (Table VI). The solid curve in Fig. 6 is obtained for an average value $\bar{\sigma} = 0.39$ and the dashed curve for $\bar{\sigma} = 0$.

C. Diffusion at low hydrogen concentrations

Diffusion coefficients are measured using anelastic relaxation (Gorsky effect)⁴⁹ by means of a capacitance apparatus described by Verbruggen *et al.*⁵⁰

In Figs. 7–9 diffusion coefficients are plotted for $\text{Ti}_{1-y}\text{V}_y$ alloys (with $y = 0.93, 0.82, 0.69, 0.62$), at different hydrogen concentrations as a function of temperature. In this section we shall restrict ourselves to the diffusion data obtained at low hydrogen concentrations ($c \sim 0.003$, i.e., 1.8 at. % H), which are plotted together with literature data for pure V and β -Ti in Fig. 7. The concentration dependence of the diffusion coefficients (Figs. 8 and 9) is discussed in Sec. V D.

The Arrhenius plots in Fig. 7 yield almost straight lines. To represent our experimental data and to make a comparison with literature data, the apparent activation energy E_{act}^a and prefactor D_a^0 are determined from a least-squares fit to the data (Table VI). In Fig. 10 the apparent activation energy for diffusion E_{act}^a is plotted as a function of alloy composition, together with data from Tanaka *et al.*²⁰ The curves in Fig. 7 are calculated by Eq. (2) using the experimental data tabulated in Tables I–VI.

We shall now discuss in detail the determination of the

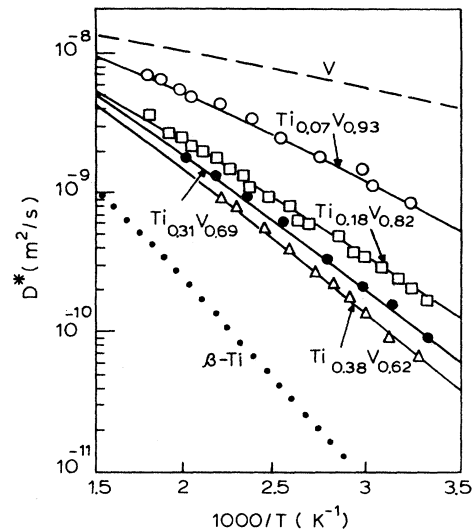


FIG. 7. Chemical diffusion coefficient D^* obtained from Gorsky effect measurements for various $\text{Ti}_{1-y}\text{V}_y$ alloys as a function of temperature. Dashed line, pure V; dotted line, β -Ti; open circles, $\text{Ti}_{0.07}\text{V}_{0.93}$ with $c = 0.002$; squares, $\text{Ti}_{0.18}\text{V}_{0.82}$ with $c = 0.0026$; solid circles, $\text{Ti}_{0.31}\text{V}_{0.69}$ with $c = 0.0033$; triangles, $\text{Ti}_{0.38}\text{V}_{0.62}$ with $c = 0.0028$; and $c = N/M$, the number of hydrogen atoms divided by the total number of sites. The solid curves are calculated diffusion coefficients using Eq. (2).

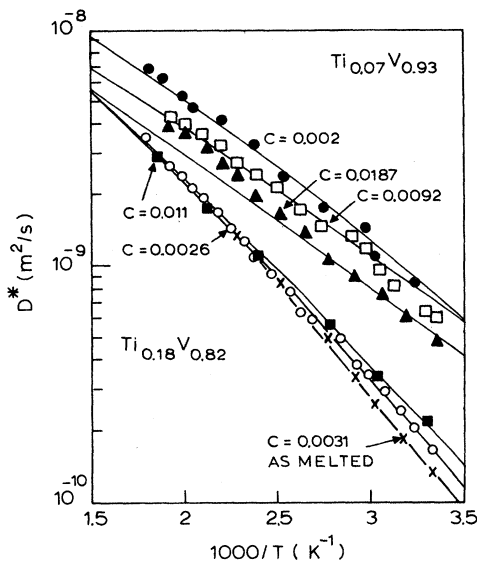


FIG. 8. Chemical diffusion coefficient D^* for $\text{Ti}_{0.07}\text{V}_{0.93}$ and $\text{Ti}_{0.18}\text{V}_{0.82}$ as a function of temperature for different hydrogen concentrations. ($\text{Ti}_{0.07}\text{V}_{0.93}$: solid circles, $c=0.002$; squares, $c=0.0092$; triangles, $c=0.0187$. $\text{Ti}_{0.18}\text{V}_{0.82}$: open circles, $c=0.0026$; solid squares, $c=0.011$). To demonstrate the influence of short-range order, D^* was also determined for an as-melted $\text{Ti}_{0.18}\text{V}_{0.82}$ sample ($c=0.0031$, crosses) with clear indications of Ti clusters by EMP analysis. As expected, the as-melted $\text{Ti}_{0.18}\text{V}_{0.82}$ sample (crosses) shows a larger (apparent) activation energy for diffusion than the annealed sample (open circles). The solid curves are calculated diffusion coefficients.

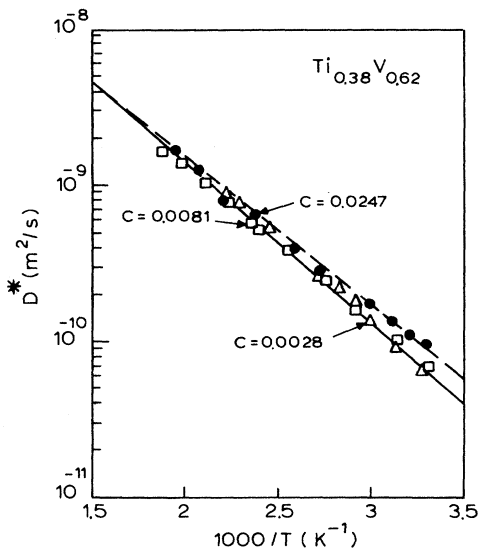


FIG. 9. chemical diffusion coefficient D^* for $\text{Ti}_{0.38}\text{V}_{0.62}$ as a function of temperature for 3 different hydrogen concentrations (triangles, $c=0.0028$; squares, $c=0.0081$; and circles, $c=0.0247$ with $c=N/M$). The solid curve is calculated for $c=0.0028$, the dashed curve for $c=0.0247$.

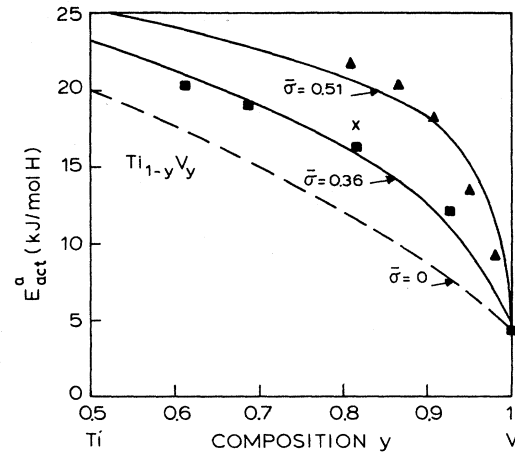


FIG. 10. Apparent activation energy for diffusion E_{act}^a as a function of composition (y) in $\text{Ti}_{1-y}\text{V}_y$ alloys. Squares, activation energies for diffusion obtained from Fig. 7; triangles, data of Tanaka and Kimura (Ref. 20). The dashed line is calculated for $\bar{\sigma}=0$, the solid curves for $\bar{\sigma}=0.36$ ($c=0.003$, temperature interval 300–525 K), respectively, $\bar{\sigma}=0.51$ ($c=0.001$, temperature interval 200–400 K). The as-melted $\text{Ti}_{0.18}\text{V}_{0.82}$ sample (cross) shows a larger activation energy for diffusion due to a larger short-range order ($\sigma=0.44$).

various parameters entering Eq. (2). The activation energy $E_{ij}(c)$ is split up (as for the pure bcc metals) into a concentration independent part, E_{ij} , and a concentration dependent part, $E(c)=Ec$, with E a constant [so $E_{ij}(c)=E_{ij}+E(c)$]. The concentration dependence of the activation energy in pure V [$E(c)=83.3c$ in kJ/mol H and $c=N/M$]⁵¹ is relatively high, compared with other bcc metals. However, for the hydrogen concentrations to be discussed in this part ($c\sim 0.003$) the concentration dependence of $E_{ij}(c)$ can be neglected. The concentration-independent part is then given by $E_{ij}=Q_{ij}-\Delta\bar{H}_i(y)$, with Q_{ij} the saddle-point energy and $\Delta\bar{H}_i(y)$ the site energy. The site energies $\Delta\bar{H}_i(y)$ are calculated with the embedded cluster model (Sec. III, Fig. 2), depending on σ via Eq. (14). The saddle-point energy Q_{ij} in pure V is -25.2 kJ/mol H,¹¹ and in β -Ti -27.2 kJ/mol H. The difference of 2 kJ/mol H in saddle-point energies is much smaller than the difference of ~ 25 kJ/mol H in the site energies of the pure metals. In $\text{Nb}_{1-y}\text{V}_y$ alloys, with pure Nb having a saddle-point energy of -25.1 kJ/mol H, a constant saddle-point energy is found as a function of alloy composition.¹¹ Considering the above arguments and the fact that Nb and Ti have almost the same lattice constants, Q_{ij} is assumed to be constant as a function of alloy composition in the $\text{Ti}_{1-y}\text{V}_y$ alloy system. The average value $Q=-25.7$ kJ/mol H is thus taken for the composition range of our alloys.

The probabilities q_{ij} to find sites of type j next to sites of type i are calculated using the expressions in Table II, which are derived for tetrahedral sites in a bcc crystal structure. The probabilities p_{AAAA} , etc., are calculated with the cluster model in Sec. IV B. The blocking factors

s_j are calculated by means of the expressions in Table I, which are derived in the Appendix of Ref. 11.

The long-range hydrogen-hydrogen interaction $f(c)$ for the alloys is simply interpolated between the values for $f(c)$ of pure V and β -Ti (Table V) for reasons discussed in Sec. VB. At low hydrogen concentrations ($c \sim 0.003$) the influence of $f(c)$ on the diffusion data is small.

Correlation effects are not expected ($f_I \sim 1$) in $Ti_{1-y}V_y$ alloys for hydrogen concentrations smaller than ~ 0.05 (30 at. % H).³³ The prefactors D_{ij}^0 depend on alloy concentration and, in principle, also on sites i and j . No experimental information is available, however, on this site dependence. As in the $Nb_{1-y}V_y$ alloy system, a good agreement with experimental diffusion coefficients was obtained by assuming site-independent prefactors $D^0 = D_{ij}^0$. We make here the same assumption and take a constant D^0 depending only on alloy composition.¹¹

For $\sigma > 0$, the site distribution p_j depends on the short-range order σ via Eqs. (17a)–(17c).

All parameters entering Eq. (2) have now been discussed. The only unknown parameters, which have to be determined from a fit to the experimental data in Figs. 7 and 10, are D^0 and the short-range-order parameter σ . The prefactors D^0 do not influence the (apparent) activation energy E_{act}^a . Therefore, the short-range order σ is determined from a fit to the slope of the curves in Fig. 7, or equivalently to E_{act}^a in Fig. 10 for all alloys. The short-range order, σ , found in our samples, is tabulated in Table VI. In Fig. 10 the solid curve is drawn for $\bar{\sigma} = 0.36$, the average short-range order for the alloys used in the experiments, the average short-range order in the alloys of Tanaka *et al.*²⁰ (Fig. 10) is $\bar{\sigma} = 0.51$.

Using σ listed in Table VI, the prefactors D^0 are determined from fits to the chemical diffusion coefficients in Fig. 7 (solid curves). In contrast to the apparent prefactors D_a^0 , the D^0 more or less interpolate between $D^0 = 3.1 \times 10^{-8}$ m²/s for V and $D^0 = 19.5 \times 10^{-8}$ m²/s for β -Ti,⁵² indicating a gradual change in jump distance and lattice vibration frequency. The same behavior was observed before in $Nb_{1-y}V_y$ alloys.¹¹

D. Diffusion at high hydrogen concentrations

In Sec. VC the chemical diffusion coefficients were calculated at low hydrogen concentrations using Eq. (2). The prefactors D^0 and the short-range order σ were determined independently from fits to the experimental data.

At high hydrogen concentrations, the concentration dependence of the activation energy, $E(c)$, and the hydrogen-hydrogen interaction, $f(c)$, become important. As these functions are not known for the $Ti_{1-y}V_y$ alloys, we have to determine them from the concentration dependence of the chemical diffusion coefficients in Fig. 8 for $Ti_{0.07}V_{0.93}$ and $Ti_{0.18}V_{0.82}$ and in Fig. 9 for $Ti_{0.38}V_{0.62}$. The hydrogen-hydrogen interaction $f(c)$ is expected to interpolate between the $f(c)$ for pure V and β -Ti (Table V) as discussed in Sec. VB. The concentration dependence of the activation energy $E(c)$ for pure β -Ti, however, has not been determined. In V, $E(c) = 83.3c$, and in

Nb, $E(c) = 65.1c$ in kJ/mol H.⁵¹ Considering the dependence of $E(c)$ on the lattice parameter and the much weaker H-H interaction in β -Ti compared to Nb (due to the smaller bulk modulus in β -Ti), $E(c)$ in β -Ti is estimated to be of the order of ~ 20 kJ/mol H.

The best fits to the chemical diffusion coefficients D^* in Fig. 8 for $Ti_{0.07}V_{0.93}$ as a function of temperature and hydrogen concentration are obtained for $E(c)$ and $f(c)$ interpolated between the values for pure V and β -Ti. For $f(c)$ the full expression $f(c) = A_1c + A_2c^2 + A_3c^3 + A_4c^4$ in pure V and the first-order expression $f(c) = A_1c$ in β -Ti are used (Table V, experimental data). For $c = 0.0325$ (i.e., 19.5 at. % H) in Fig. 11, the fit to the experimental data is not perfect (solid curve). The best fit was obtained for an interpolated $f(c)$ and $E(c) = 32c$, which indicates that at high hydrogen concentrations the concentration dependence $E(c)$ changes, as was also observed for pure V, Nb, and Ta.⁵¹ The disagreement is not considered to be serious when we study the influence of the various parameters in Eq. (2) at this hydrogen concentration. One by one we changed the parameters $E(c)$, $f(c)$, and σ to study their influence on the chemical diffusion coefficients D^* . Without short-range order ($\sigma = 0$, dotted curve) the diffusion coefficients D^* decrease strongly at low temperatures (critical slowing down). The effective H-H interactions are no longer compensated for $\sigma = 0$ by the (increased) disorder in the lattice. Without $f(c)$ and $E(c)$ the dashed line is obtained. The parameters $E(c)$, $f(c)$, and σ can change the chemical diffusion coefficients D^* by approximately 2 orders of magnitude, whereas the deviation between calculated data (solid curve) and experimental data (lozenges) is relatively small.

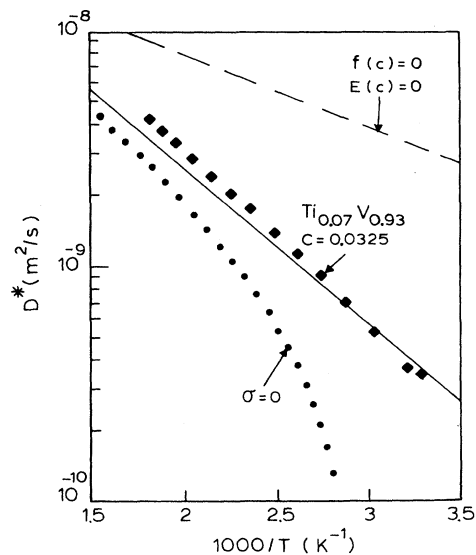


FIG. 11. Chemical diffusion coefficients D^* for $Ti_{0.07}V_{0.93}$ and $c = 0.0325$ as a function of temperature (lozenges). The solid curve is the best fit to the data, with $E(c) = Ec$ and $f(c) = A_1c$ as fit parameters. The dashed curve for $f(c) = 0$ and $E(c) = 0$, and the dotted curve for $\sigma = 0$, to demonstrate the influence of the various parameters.

In Fig. 8 the chemical diffusion coefficients D^* for $\text{Ti}_{0.18}\text{V}_{0.82}$ are plotted as a function of temperature and hydrogen concentration. The D^* show an interesting behavior as a function of the hydrogen concentration at low temperatures. The diffusion coefficients for $c=0.011$ are larger than for $c=0.0026$. In a pure metal D^* always decreases with increasing hydrogen concentration, due to hydrogen-hydrogen interactions $f(c)$, due to $E(c)$, and due to blocking. All these effects are compensated in the $\text{Ti}_{0.18}\text{V}_{0.82}$ alloy by *site filling*. With increasing hydrogen concentration, sites with higher energy are occupied, thereby lowering the activation energy for diffusion and increasing the diffusion coefficients D^* . The best fits to the experimental data for $\text{Ti}_{0.18}\text{V}_{0.82}$ in Fig. 8 are obtained for $E(c)=24c$ and $f(c)=-58c$, in kJ/mol H and $c=N/M$, with N the total number of hydrogen atoms divided by the total number M of interstitial sites.

In Fig. 9 the chemical diffusion coefficients D^* for $\text{Ti}_{0.38}\text{V}_{0.62}$ are plotted for three hydrogen concentrations. Again D^* is observed to increase with hydrogen concentration in contrast to D^* in pure metals. The best fits to the experimental data in Fig. 9 are obtained for negligible concentration dependences for $E(c)$ and $f(c)$.

In the past there have been some reports on an (apparent) weakening of H-H interactions in disordered alloys, based on the weak dependence of the enthalpy of solution $\Delta\bar{H}(y)$ on hydrogen concentration and/or the increase in the solubility limit.^{48,53} In Ref. 25 it is clearly shown that these effects do not indicate a weakening of $f(c)$ in disordered alloys but are merely due to a compensation of $f(c)$ by site filling effects.

The *observed weakening* of $E(c)$ and $f(c)$ in $\text{Ti}_{0.18}\text{V}_{0.82}$

and $\text{Ti}_{0.38}\text{V}_{0.62}$ alloys is therefore probably not simply related to the *disorder*, but to the *short-range order*, i.e., to the clustering observed in these alloys.

VI. DISCUSSION AND CONCLUSIONS

In the Introduction, a number of indications have been given for the existence of short-range order in the $\text{Ti}_{1-y}\text{V}_y$ alloy system. In Secs. V B, V C, and V D, solution and diffusion data of hydrogen in $\text{Ti}_{1-y}\text{V}_y$ alloys are compared with calculated values, and with experimental data obtained by other workers. In previous papers, always an excellent agreement was obtained between calculated and experimental enthalpies of solution,²⁵ interaction energies,²⁵ and diffusion coefficients,¹¹ in alloys containing either V or β -Ti. Assuming the existence of short-range order in the $\text{Ti}_{1-y}\text{V}_y$ alloys, a good agreement is obtained between calculated and experimental data, as a function of temperature, hydrogen concentration, and alloy composition.

As a final check that short-range order results in a higher activation energy for diffusion, due to an increase in the number of Ti_4 sites and a decrease in site energies, we measured D^* in an "as-melted" $\text{Ti}_{0.18}\text{V}_{0.82}$ sample (same batch as annealed sample, $c=0.0031$, EMP analysis shows $y=0.82\pm 0.02$). In Figs. 8 and 10 the diffusion coefficients D^* and apparent activation energy of the annealed and as-melted $\text{Ti}_{0.18}\text{V}_{0.82}$ sample are compared. The increase in the activation energy in the as-melted sample is consistent with the observation of Ti clusters by EMP analysis.

In Table VII the average short-range order found in

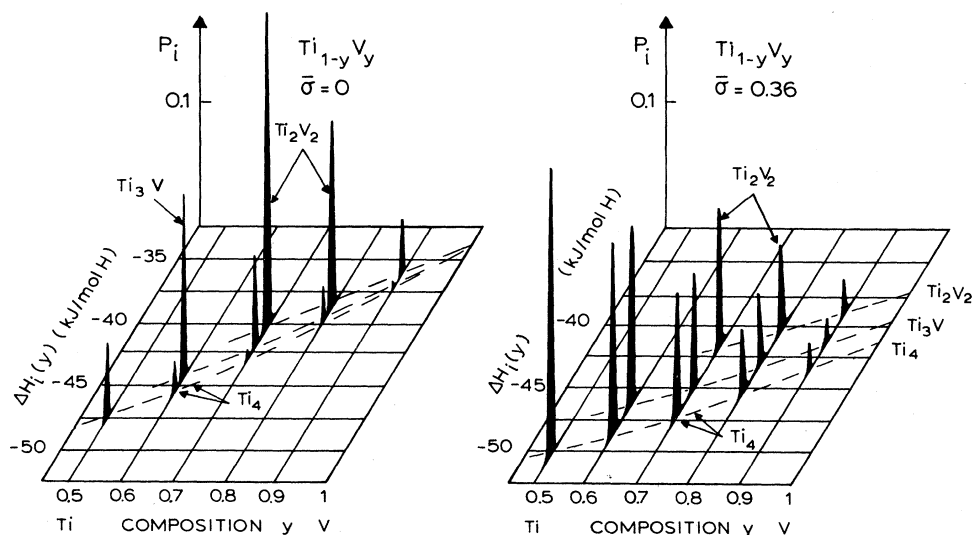


FIG. 12. Site fractions (p_i) as a function of alloy composition y and as a function of site energies $\Delta\bar{H}_i(y)$ for various $\text{Ti}_{1-y}\text{V}_y$ alloys, with short-range order $\bar{\sigma}=0.36$ and without short-range order $\bar{\sigma}=0$ (binomial site distribution). Only the sites with lowest energy (Ti_2V_2 , Ti_3V , and/or Ti_4 sites) are shown. The sites with lowest energies accommodate most of the hydrogen atoms, and therefore have a large influence on the diffusion coefficients of hydrogen in the alloys, or on the enthalpy of solution in the alloys. As is clearly observed, the number of sites with lowest energy increases strongly with increasing short-range order. The energy of the different sites is also shifted to lower values due to the clustering of the Ti (and V) atoms.

TABLE VII. Average short-range-order parameters $\bar{\sigma}$ determined from the activation energy for diffusion or the enthalpies of solution for hydrogen in various $\text{Ti}_{1-y}\text{V}_y$ alloys (Figs. 1 and 6). From left to right in columns, the authors, the temperature interval in the experiments, the average hydrogen concentration, the annealing temperature T_a for the samples, the average short-range order $\bar{\sigma}$ in the experiment, and the variation in the short-range order $\Delta\bar{\sigma}$ (between different alloy compositions).

Source	T (K)	$\bar{\sigma}$	T_a (K)	$\bar{\sigma}$	$\Delta\bar{\sigma}$
This work	300–525	0.003	1900	0.36	0.04
Takana <i>et al.</i> ^a	200–400	0.001	1270	0.51	0.06
Pine <i>et al.</i> ^b	310–480	0.001	1300–1800	0.40	0.05
Peterson <i>et al.</i> ^c	230–473	0.001		0.41	0.06
Peterson <i>et al.</i> ^d	297–473	0.01		0.39	0.06

^aReference 20.

^bReference 23.

^cReference 21.

^dReference 48.

our samples is compared with the short-range order in samples of other authors (determined from solution and diffusion data). There is a correlation between annealing temperature, activation energy for diffusion, and short-range order in the alloys. In the alloys of Tanaka *et al.*,²⁰ with a low annealing temperature T_a of 1270 K, the largest short-range order $\bar{\sigma}=0.51$ is found, in agreement with their observations of Ti clusters in V-rich alloys. In our alloys, with $\bar{\sigma}=0.36$ and annealing temperature $T_a=1900$ K, we do not observe clustering by EMP analysis.

In Fig. 12 the influence of the short-range order $\bar{\sigma}$ on the site energies and site fractions in $\text{Ti}_{1-y}\text{V}_y$ alloys is demonstrated. Due to the short-range order $\bar{\sigma}=0.36$, the site energies decrease much more rapidly and the number of Ti_4 sites increases much more rapidly in alloying Ti to V than for $\bar{\sigma}=0$.

We summarize now the main results of this work. Diffusion coefficients have been measured in concentrated disordered $\text{Ti}_{1-y}\text{V}_y$ alloys as a function of temperature, hydrogen concentration, and alloy composition. Diffusion is described by a model, incorporating site-dependent, activation energies, effective H-H interactions, and selective-blocking factors, generalized for alloys with short-range order. Site energies have been calculated using the embedded cluster model. The influence of short-range order on the site energy and site distribution has been established. For $\sigma < 0$ the chain model and for $\sigma > 0$ the cluster model is in good agreement with Monte Carlo calculations. For the first time the enthalpies of solution and diffusion coefficients in $\text{Ti}_{1-y}\text{V}_y$ alloys are calculated as a function of composition (y), hydrogen concentration, and temperature. A good agreement between calculated and experimental data is obtained. The short-range order in the $\text{Ti}_{1-y}\text{V}_y$ alloys is

determined quantitatively both from solubility and diffusion data. The determination of local lattice constants in $\text{Nb}_{1-y}\text{V}_y$ alloys,¹⁴ the short-range order in $\text{Mo}_{1-y}\text{Ti}_y$ alloys,²⁵ and, in this paper, in $\text{Ti}_{1-y}\text{V}_y$ alloys from solubility and diffusion data, demonstrates that hydrogen in “disordered” alloys can be used as a local probe for the physical and/or chemical structure of an alloy.

ACKNOWLEDGMENTS

This investigation was part of the research program of the Stichting voor Fundamenteel Onderzoek der Materie (FOM), which is financially supported by the Nederlandse Organisatie voor Wetenschappelijk Onderzoek (NWO).

APPENDIX

Assuming that the influence of one A and B atom cancels each other [Eq. (19)], the site fractions $p(i, \sigma)$ [Eqs. 17(a)–17(c)] for tetrahedral interstitial sites $A_{4-i}B_i$ in a bcc alloy $A_{1-y}B_y$ may be given by the following relations:

$$p(i=0, \sigma) = p_{APAAA} p_{AAAA} p_{AAAAA},$$

$$p(i=1, \sigma) = p_{APAAP} p_{AAAP} p_{AAAB} + p_{APAA} p_{AAB} p_{AA} \\ + p_{APAB} p_{APAA} + p_{BPBAP} p_{APAA},$$

$$p(i=2, \sigma) = p_{APAA} p_{AAB} p_{AB} + p_{APAB} p_{APAB} \\ + p_{BPBAP} p_{APAB} + p_{BPBAP} p_{BPBA} \\ + p_{BPBB} p_{BBAP} p_{BA} + p_{APAB} p_{BPBPBA}$$

[$p(i=3, \sigma)$ and $p(i=4, \sigma)$ are obtained from $p(i=1, \sigma)$ and $p(i=0, \sigma)$ by exchanging A and B].

¹Hydrogen in Metals I and II, Vols. 28 and 29 of *Topics in Applied Physics*, edited by G. Alefeld and J. Völkl (Springer-Verlag, Berlin, 1978).

²Y. Fukai and H. Sugimoto, *Adv. Phys.* **34**, 263 (1985).

³C. P. Flynn and A. M. Stoneham, *Phys. Rev. B* **1**, 3966 (1970).

⁴H. Teichler and A. Klamt, *Phys. Lett.* **108A**, 281 (1985).

⁵D. Emin, M. I. Baskes, and W. D. Wilson, *Phys. Rev. Lett.* **42**, 791 (1979).

- ⁶R. Griessen and T. Riesterer, in *Hydrogen in Intermetallic Compounds I*, Vol. 63 of *Topics in Applied Physics*, edited by L. Schlapbach (Springer-Verlag, Berlin, 1988), pp. 219–284.
- ⁷R. A. Oriani, *Acta Metall.* **18**, 147 (1970).
- ⁸M. Koiwa, *Acta Metall.* **22**, 1259 (1974).
- ⁹R. Kirchheim, *Acta Metall.* **30**, 1069 (1982).
- ¹⁰R. Griessen, *Phys. Rev. B* **27**, 7575 (1983).
- ¹¹R. C. Brouwer, E. Salomons, and R. Griessen, *Phys. Rev. B* **38**, 10 217 (1988).
- ¹²R. Griessen and A. Driessen, *J. Less-Common Met.* **103**, 245 (1984).
- ¹³R. Griessen, in *Hydrogen in Disordered and Amorphous Solids*, edited by G. Bambakidis and R. C. Bowman (Plenum, New York, 1986), pp. 153–172.
- ¹⁴R. Feenstra, R. Brouwer, and R. Griessen, *Europhys. Lett.* **7**, 425 (1988).
- ¹⁵S. Froyen and C. Herring, *J. Appl. Phys.* **52**, 7165 (1981).
- ¹⁶S. C. Moss and B. L. Averbach, in *Small Angle Scattering*, edited by H. Braumberger (Gordon and Breach, New York, 1967), p. 335.
- ¹⁷J. Vrijen and S. Radelaar, *Phys. Rev. B* **17**, 409 (1978).
- ¹⁸P. Eisenberger and B. Lengeler, *Phys. Rev. B* **22**, 3551 (1980).
- ¹⁹M. Mrowietz and A. Weiss, *Ber. Bunsenges. Phys. Chem.* **89**, 49 (1985).
- ²⁰S. Tanaka and H. Kimura, *Trans. Jpn. Inst. Met.* **20**, 647 (1979).
- ²¹P. S. Rudman, *Acta Metall.* **12**, 1381 (1964).
- ²²D. T. Peterson and H. M. Herro, *Metall. Trans.* **18A**, 249 (1987).
- ²³D. J. Pine and R. M. Cotts, *Phys. Rev. B* **28**, 641 (1983).
- ²⁴T. Eguchi and S. Morozumi, *J. Jpn. Inst. Met.* **41**, 795 (1977).
- ²⁵R. C. Brouwer and R. Griessen, *Phys. Rev. B* **40**, 1481 (1989).
- ²⁶R. B. McLellan, *Acta Metall.* **30**, 317 (1982).
- ²⁷M. Yoshihara and R. B. McLellan, *Acta Metall.* **34**, 1359 (1986).
- ²⁸R. B. McLellan and M. Yoshihara, *J. Phys. Chem. Solids* **48**, 661 (1987).
- ²⁹R. Kirchheim, *Acta Metall.* **35**, 271 (1987).
- ³⁰R. Kirchheim and U. Stolz, *J. Non-Cryst. Solids* **70**, 323 (1985).
- ³¹R. Kirchheim and U. Stolz, *Acta Metall.* **35**, 281 (1987).
- ³²G. Boureau, *J. Phys. Chem. Solids* **42**, 743 (1981).
- ³³G. E. Murch, in *Atomic Diffusion Theory in Highly Defective Solids*, Vol. 6 of *Diffusion and Defect Monograph Series*, edited by Y. Adda, A. D. le Claire, L. M. Slifkin, and F. H. Wöhlbier (Trans Tech, Aedermannsdorff, 1980).
- ³⁴G. E. Murch and R. J. Thorn, *Philos. Mag. A* **40**, 477 (1979).
- ³⁵G. E. Murch and R. J. Thorn, *J. Phys. Chem. Solids* **39**, 1301 (1978).
- ³⁶R. Feenstra, P. Meuffels, B. Bischof, and H. Wenzl (unpublished).
- ³⁷M. Manninen, M. J. Puska, R. M. Nieminen, and P. Jena, *Phys. Rev. B* **30**, 1065 (1984).
- ³⁸A. I. Shirley and C. K. Hall, *Acta Metall.* **32**, 49 (1984).
- ³⁹R. Griessen, *Phys. Rev. B* **38**, 3690 (1988).
- ⁴⁰R. Griessen and A. Driessen, *Phys. Rev. B* **30**, 4372 (1984).
- ⁴¹M. Cyrot and F. Cyrot-Lackmann, *J. Phys. F* **6**, 2257 (1976).
- ⁴²R. Feenstra, R. Griessen, and D. G. de Groot, *J. Phys. F* **16**, 1933 (1986).
- ⁴³K. W. Katahara, M. H. Manghnani, and E. S. Fisher, *J. Phys. F* **9**, 773 (1979).
- ⁴⁴D. Nguyen Manh, D. Mayou, A. Pasturel, and F. Cyrot-Lackman, *J. Phys. F* **15**, 1911 (1985).
- ⁴⁵H. K. Adenstedt, J. R. Pequignot, and J. M. Raymer, *Trans. Am. Soc. Met.* **44**, 990 (1952).
- ⁴⁶M. Hansen and K. Anderko, in *Constitution of Binary Alloys*, 2nd ed. (McGraw-Hill, New York, 1958), p. 1240.
- ⁴⁷T. Hagi, Y. Sato, M. Yasuda, and K. Tanaka, *Trans. Jpn. Inst. Met.* **28**, 198 (1987).
- ⁴⁸D. T. Peterson and S. O. Nelson, *Metall. Trans.* **16A**, 367 (1985). The data were recalculated, with the experimental data at 223 K left out, which shows a systematic deviation (Fig. 10 of this Ref.). The data are corrected for differences in H concentration if necessary. The enthalpies of solution for the alloys were measured *relative* to pure V. In order to compare the data with the best literature values, all data were shifted by +3.6 kJ/mol H.
- ⁴⁹J. Völkl, *Ber. Bunsenges. Phys. Chem.* **76**, 797 (1972).
- ⁵⁰A. H. Verbruggen, C. W. Hagen, and R. Griessen, *J. Phys. F* **14**, 1431 (1984).
- ⁵¹J. E. Kleiner, E. H. Sevilla, and R. M. Cotts, *Phys. Rev. B* **33**, 6662 (1986).
- ⁵²R. J. Wasilewski and G. L. Kehl, *Metallurgia* (1954) 225.
- ⁵³J. F. Lynch, J. J. Reilly, and F. Millot, *J. Phys. Chem. Solids* **39**, 883 (1978).
- ⁵⁴V. L. Moruzzi, J. F. Janak, and A. R. Williams, in *Calculated Electronic Properties of Metals* (Pergamon, New York, 1978).
- ⁵⁵K. Gschneider, in *Solid State Physics*, edited by F. Seitz and D. Turnbull (Academic, New York, 1964), Vol. 16, p. 275.
- ⁵⁶*Handbook of Chemistry and Physics*, 59th ed., edited by R. C. Weast and M. J. Astle (CRC, West Palm Beach, Florida, 1978), pp. E81–E83.